

GUIDED WAVE INTERPRETATION FOR INTEGRATED VEHICLE HEALTH MANAGEMENT SENSORS

Jill Bingham
Nondestructive Evaluation Laboratory
Department of Applied Science
The College of William and Mary

Abstract

Integrated Vehicle Health Management (IVHM) combines the use of onboard sensors with artificial intelligence algorithms to automatically identify and monitor structural health issues. A fully integrated approach to IVHM systems demands an understanding of the sensor output relative to the structure, along with sophisticated prognostic systems that automatically draw conclusions about structural integrity issues. Ultrasonic guided wave methods allow us to examine the interaction of the signals within key structural components. Since they propagate relatively long distances within plate- and shell-like structures, guided waves allow inspection of greater areas with fewer sensors. In order to interpret the signals that we receive from transducers we look not only at the wave mechanics but also the signal processing using the dynamic wavelet fingerprinting technique to deliver the information in a form that does not require extensive knowledge of the guided wave physics.

Introduction

With a national fleet of aging aircraft and infrastructure, safety will become an increasing priority. IVHM promises low-cost, real-time sensing/inspection methods to detect damage before catastrophic failure. Ultrasonic guided waves, Lamb waves, allow for large areas of plate-like structures, such as airframes, storage tanks and pipes to be inspected with fewer sensors than conventional point by point measurements since they interrogate the entire region between sensor pairs¹²³⁴. By understanding

the waveguide physics we can develop systems that are tailored to the application at hand. However due to the complicated nature of guided wave propagation, we also develop algorithms that automatically analyze the waveforms and present the critical information in a form that doesn't require users to have extensive knowledge of the physics. The propagation of the Lamb wave modes depends on the vibrational frequency along with the thickness and material properties of the structure. So variations in the waveforms can be used to assess the integrity of the structure for flaws such as disbands, corrosion and cracks that represent changes in effective thickness and/or local material properties.

The research presented in this paper deals with our preliminary efforts to understand the wave propagation in airframe stringers and their interaction with corrosion and thickness loss flaws. We work our way through a propagation distance study, an incremental thickness loss experiment and finally an accelerated corrosion test. In each case we employ the dynamic wavelet fingerprinting technique (DWFT) to extract mode arrivals⁵.

Experimental Details

This set of studies was conducted on sample aluminum airframe stringers that are 1m in length and have a "T" cross-section. The original flange thickness was 1.6mm. We use piezoelectric contact transducers in a pitch-catch arrangement to inspect the samples. The transmitting transducer excites Lamb wave modes that are then recorded by the receiving transducers. Since the Lamb

wave modes are dispersive, the presence of a flaw shifts the arrival times and amplitudes of the Lamb wave modes received. Figure 1 shows the dispersion curves for Lamb waves in aluminum, depicting how a change in the thickness of the material results in a change in the group velocity of the mode.

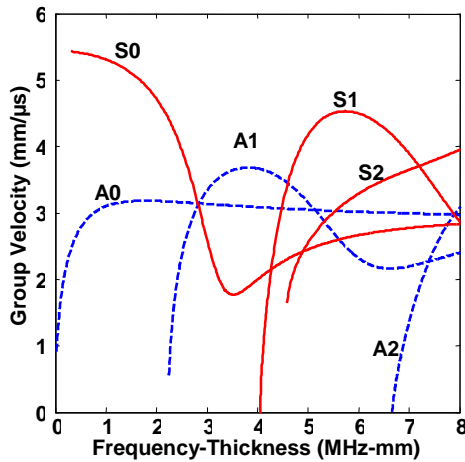


Figure 1: Lamb wave dispersion curves for an aluminum plate. A change in thickness of the material results in a change in arrival time of the mode since its group velocity changes.

By exciting the transducers at lower frequencies we ensure that the frequency thickness product is below the cut-off frequencies for the higher modes, making the waveforms less complicated. In the instance of the 1.6mm thick aluminum stringer, this means using excitation frequencies of 1.4 MHz or lower. In this region of the dispersion curve any thickness loss will be represented as a increase in the group velocity of the first arriving, S0 mode, while the second mode, the A0 mode will have a relatively small change in arrival over the same change in thickness.

Dynamic Wavelet Fingerprinting Technique (DWFT)

Due to the need to extract multiple mode arrivals from the complicated time-series data received by the transducers, we have found that joint time-frequency methods are commonly used⁶. They have the ability to

isolate individual spectral components while retaining their absolute relationships in time domain. Specifically, we have found that using the wide versatility of wavelet transformations is perfect for this application. By choosing a mother wavelet that optimally represents a signal feature, i.e. a mode, we can better isolate features of interest in time-scale representation. Another added bonus to this approach is that the transformation takes the 1D signal and transforms it into a 2D image that allows us to work with 2D image processing operations. Our DWFT renders the time-series signal as binary contour plots of the wavelet transform coefficients. The resulting fingerprint-like image is amenable to computerized interpretation for automated extraction of signal features of interest.

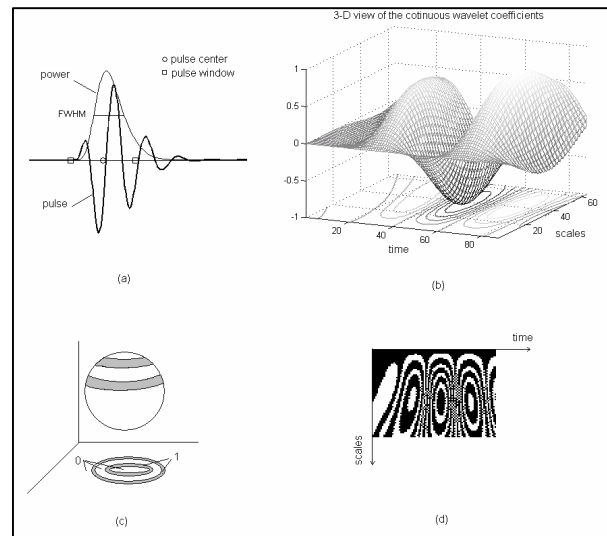


Figure 2: Wavelet fingerprints generation. (a) Ultrasound pulse; (b) 3D view of the wavelet coefficients and its contour; (c) slice projection; (d) the dynamic wavelet fingerprint of (b).

Figure 2 illustrates how the wavelet fingerprints are formed. An isolated ultrasonic pulse is shown in (a) along with a standard surface plot (b) of the corresponding continuous wavelet coefficients. In (b) we also see the coefficients displayed as a traditional contour plot underneath the surface plot. To form a wavelet fingerprint, we use the “thick contours” shown in (c). The

wavelet coefficients are first normalized into the range of [0, 1], and then equal slices of the 3D-coefficient surface are projected back onto the time-scale plane. This results in the black and white, 2D representation shown in (d) which we refer to as the wavelet fingerprint.

Results and Discussion

Propagation Distance Study

Part of the difficulty of an IVHM solution is looking into the tradeoffs between how few sensors are needed to cover an area of the structure, while still interrogating the region at the required level detail. To tackle this problem we did a study of the propagation of the waves down the length of the stringer. Our approach was to record waveforms with increasing propagation lengths to follow the mode dispersion and quality of the signal. The set of graphs below in figure 3 shows the waveforms recorded for propagation lengths of 50, 60, 70, 80, and 90 cm respectively.

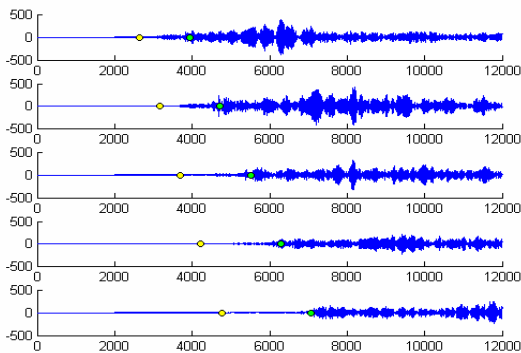


Figure 3: Raw waveforms recorded from aluminum stringer with increasing propagation lengths (50, 60, 70, 80, 90 cm top to bottom). Yellow and green dots show the expected arrival points for the S0 and A0 modes respectively, derived from the dispersion curve using the 1.4 MHz excitation frequency.

Notice that the waveforms have very complicated structures. Using the yellow and green dots as approximate reference points for the arrival times of the S0 and A0 modes respectively, we see that we cannot use simple threshold methods to extract the modes. However, if we pass the waveforms through a discrete stationary wavelet transform filter and remove a few levels of detail we can start to

identify the modes of interest in our signals. Shown below in figure 4 is the same signal set as above after being passed through the filter.

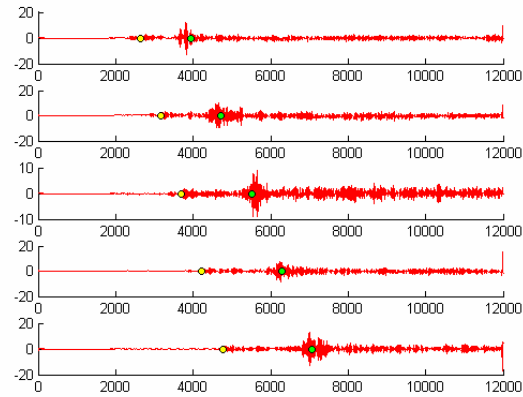


Figure 4: Result from passing the waveforms in figure 3 through a discrete stationary wavelet transform filter and removing a few levels of detail.

Enveloping the filtered signals gives us our final input to use with the DWFT. In this case we wanted to identify the first two modes and see their separation in time for the increasing propagation lengths.



Figure 5: Resulting fingerprints from employing the DWFT on the enveloped, filtered signals found in figure 3. Note the triangular feature to left is an artifact that shows the beginning of the envelope.

In the above figure 5, the first two modes are clearly identified using the DWFT. As the propagation distance increases we can see the faster S0 mode separating itself from the second arriving A0 mode. It is also useful to notice that the two modes have different structures in their fingerprint representation. The S0 mode is a singlet form while the A0 is

represented as a doublet. Using this analysis we determined that it is possible to interrogate the entire length of the sample stringers using one pitch-catch pair of transducers. In this configuration we do not see a deterioration of the ultrasonic signal.

Accelerated Corrosion Test

In order to study the interaction between the guided waves and corrosion on the samples we set up an accelerated corrosion test in which we introduced corrosion on a portion of the surface of the flange on the stringer. The accelerated corrosion test came from an ASTM standard test method known as the EXCO test⁷. For the tests we used a spike excitation with 1 MHz shear contact transducers. With the transducers in pitch-catch configuration we placed the transducers 10 cm from each end of the stringer. This was to reduce the effect of reflections off of the ends of the sample when recording the waveforms during the corrosion test. After taking a baseline waveform we fluid loaded 46 cm of the 80 cm propagation length with the EXCO solution to start the corrosion process. During the process the sample was monitored, taking periodic waveforms. The time-series signals were then treated in the same fashion as was use above in the propagation distance study. Below, figure 6, are the fingerprints generated from the baseline waveform and the waveform after the 46 hour exposure time and the corrosion products were wiped off of the sample.



Figure 6: Fingerprints generated from the start (1) and end (30) of the corrosion study by the DWFT.

In these fingerprints we see the first two modes with the same structure as in the propagation study. The first arriving S0 mode is a singlet while the A0 has more of a doublet structure. It is clearly seen that the highly dispersive S0 mode speeds up with the

material loss due to the corrosion process while the A0 has relatively the same arrival time as would be expected according to the dispersion curves in figure 1.

Incremental Thickness Milling

While the accelerated corrosion test let us see how the guided waves behave in a corrosion situation we also wanted to study the interaction with the material loss in a more controlled fashion. So instead of the EXCO solution we used a milling machine to simulate the effect so corrosion by incrementally decreasing the thickness of the flange. Whereas it is difficult to determine material properties and thickness of the sample mid accelerated corrosion test, here we know precisely how much material we are removing at each step. We have examined the effect of 13 steps of removing material. The clean T-stringer is 1m long and the bottom flange is 20mm wide on each side of the web. So sitting on the table it looks like an upside down “T”. The milling increments were taken from the middle of the bottom flange. Table 1 below contains the dimensions. Whenever the length or width dimensions increase the new cuts are less severe at first then we stepped down until the entire region is the same depth.

Step	From left end (mm)	From flange side (mm)	Width (mm)	Length (mm)	Thickness (mm): Method 1	Method2*
1					1.578	1.645
2	475	10	11	25	1.501	
3	475	10	11	25	1.337	
4	475	10	11	50	1.414	
5	475	10	11	50	1.33	
6	475	0	20	50	1.504	
7	475	0	20	50	1.421	
8	475	0	20	50	1.006	1.111
9	475	0	20	76		1.602
10	475	0	20	76		1.43
11	475	0	20	77		1.318
12	475	0	20	77		1.186
13	475	0	20	77		.955

Table 1: Incremental milling step deminsions

* The micrometer was re-zeroed during the tests

For the tests the transducers were placed 10cm from the ends of the stringers again in an effort to separate the reflections from the ends out in time from the signal that we care about. So the total propagation length was 80cm with the flaw in the middle. Figure 7 below shows the signals for each of the steps. The red region of the signal indicates the windowed filtered region that was passed to the wavelet fingerprinting algorithm. This was found using the expected arrival time of the S0 mode for the clean sample.

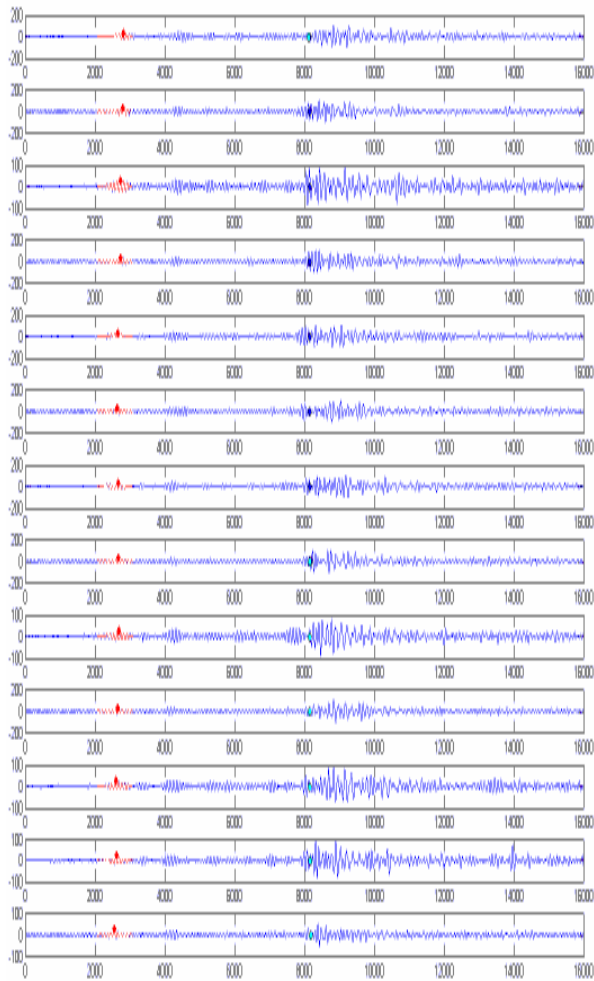


Figure 7: Waveforms from the incremental milling tests. The red portion of the time-series signal is the windowed filter region that is passed to the DWFT.

The red dots in the figure 7 indicate the arrivals of the S0 mode determined by using the fingerprint algorithm. The blue dots to the right are the expected arrival times for the

second arriving A0 mode. We decided to use only a portion of the waveform in generating the fingerprints because we wanted get arrival information from one mode at a time. Below in figure 8 are the resulting fingerprints from the windowed, filtered signal for the S0 mode. The pre-filter used here is a discrete stationary wavelet transform using the ‘coif3’ mother wavelet and it removes several levels of detail in order to de-noise the signal.

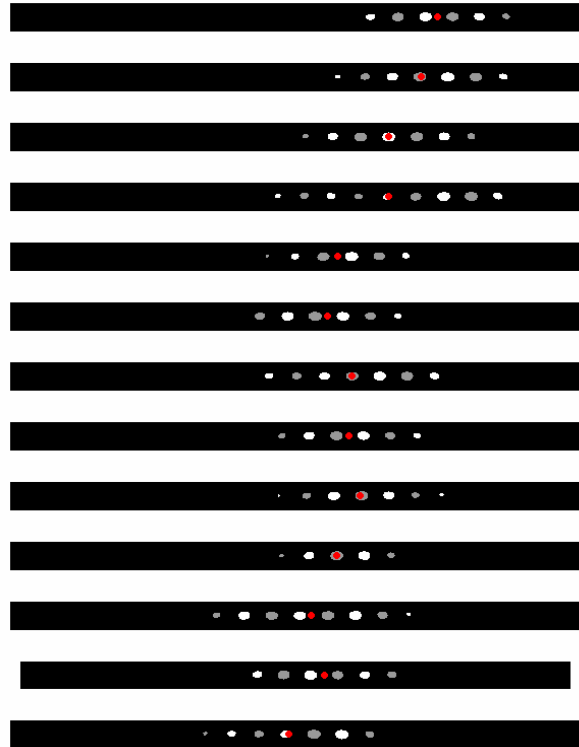


Figure 8: DWFT generated finger prints for the windowed, filtered waveforms of the S0 modes for the incremental milling test. The red dot signifies the central occurrence of the fingerprint.

The red dot locations are computed from the central occurrence of the fingerprint. Below in figure 9 you can see the definite increase in velocity of the first mode shown by the sooner arrival points of the mode. Here, another interesting point is that the middle steps where the mode arrival seems to skip around a bit more than in other places, the milling machine was used to increase the width of the flaw. This means that it is harder to determine which portion the wave is actually traveling through the thicker side that we were still

stepping or the thin side that remained the same. From here we plan to continue to look at the effects of the thinning region as it increases. The most severe flaw used here is only 9.6% of the propagating distance with a total thickness loss of 58%. Continuing in this fashion we will be able to examine less severe damage over wider areas, and from further distances away.

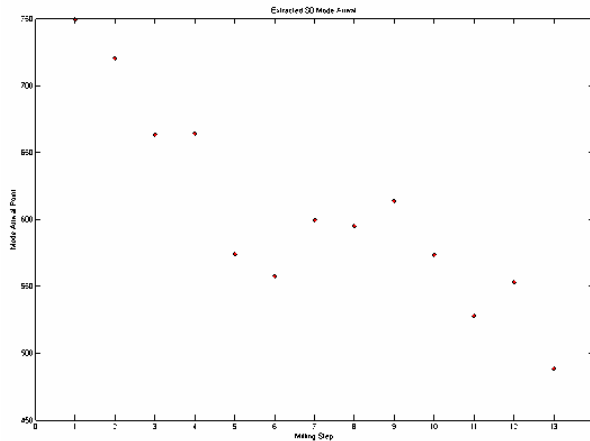


Figure 9: Extracted S0 mode arrivals from the 13 steps of the incremental milling test using the DWFT.

Conclusions

We have presented work here that shows that the DWFT is helpful in determining the propagation and arrivals of multiple guided wave modes. The wavelet fingerprints are binary images, so they are simple to store and straightforward to process digitally, and we can draw on the large scientific and technological literature in fingerprint and character recognition to develop computer algorithms that automatically identify features in them. By incorporating the details of the wave propagation into algorithms for inspection and structural health monitoring, we develop more informative and quantitative techniques.

Acknowledgements

I would like to thank Hasso Weiland of the Alcoa Technical center for providing the stringer samples and for helpful discussions.

¹ J. D. Achenbach Wave Propagation in Elastic Solids. Amsterdam: North-Holland. (1984).

² B. A. Auld, Acoustic Fields and Waves in Solids. Malabar, FL: Kreiger. (1990).

³ J. L. Rose, Ultrasonic Waves in Solid Media. Cambridge: Cambridge University Press. (1999).

⁴ J. L. Rose, "A Baseline and Vision of Ultrasonic Guided Wave Inspection Potential" Journal of Pressure Vessel Technology- Transactions of the ASME 124 (3): 273-782 (2002).

⁵ J. Hou, Kevin R. Leonard and M. Hinders, "Automatic Multi-mode Lamb Wave Arrival Time Extraction for Improved Tomographic Reconstruction" Inverse Problems 20, 1873-1888 (2004).

⁶ M. Hinders, J. Hou, "Dynamic Wavelet Fingerprint Identification of Ultrasound Signals" Materials Evaluation 60, #9 1089-1093, (2002).

⁷ ASTM International, "Standard Test Method for Exfoliation Corrosion Susceptibility in 2XXX and 7XXX Series Aluminum Alloys (EXCO Test)" Designation: G 34 – 01.